

Electronic supplementary information for

**Novel photocatalytic performance of nanocage-like MIL-125-NH<sub>2</sub>  
induced by adsorption of phenolic pollutants**

**Preparation of NC-MIL-125-NH<sub>2</sub>.** NC-MIL-125-NH<sub>2</sub> was fabricated from MIL-125-NH<sub>2</sub>. MIL-125-NH<sub>2</sub> was synthesized as the procedure below. 2-aminoterephthalic acid (0.868 mg, 4.8 mmol) was added in a mixing solvents of dry DMF (20 mL) and anhydrous CH<sub>3</sub>OH (20 mL) before the solution was ultrasonically dispersed. Then titanium(IV) isopropoxide (0.708 mL 2.4 mmol) was slowly added into the homogeneous mixture with stirring. The mixture was continuously stirred at room temperature for 30 minutes, and then transferred to a 100 mL Teflon-lined autoclave and heated at 150 °C for 15 h in an oven. Afterwards, the mixture was cooled to room temperature, and yellow powders were recovered by centrifugation and was washed several times with DMF and anhydrous methanol, respectively. After vacuum dried at 60 °C, MIL-125-NH<sub>2</sub> powders were obtained for further synthesis. And then MIL-125-NH<sub>2</sub> (200 mg) was dispersed into anhydrous C<sub>2</sub>H<sub>5</sub>OH (50 mL) by sonication. Afterwards, L-alanine (800 mg) was added into the mixture and stirred for 1 h to mix thoroughly. And then the mixture was transferred to a 100 mL Teflon-lined autoclave and heated at 176 °C for 72 h. The NC-MIL-125-NH<sub>2</sub> was collected by centrifugation and washed several times with anhydrous ethanol. After vacuum dried at 60 °C, NC-MIL-125-NH<sub>2</sub> powders were obtained for further analysis.

**Characterization of NC-MIL-125-NH<sub>2</sub>.** Scanning electron microscopy (SEM) was performed through Nano nova 450 SEM (FEI, Netherlands). Transmission electron microscopy (TEM) was performed through Tecnai G2F30 S-Twin TEM (FEI, Netherlands). Brunauer-Emmett-Teller (BET) was estimated by nitrogen adsorption-desorption at -196 °C with a NOVA-2000E surface area analyzer. X-ray diffraction (XRD) was examined using a Thermal ARL X-ray diffractometer (Thermo, France) at room temperature with Cu K $\alpha$  radiation ( $\lambda = 0.154$  nm) at a scan rate of  $0.01^\circ \text{ s}^{-1}$  in the  $2\theta$  range from 5 to 80°. The fourier transform infrared spectroscopy (FTIR) spectra were recorded in the 4000-400 cm<sup>-1</sup> region with a resolution of 4 cm<sup>-1</sup> using a Nicolet Thermo NEXUS 670. X-ray photoelectron spectroscopy (XPS) experiments were performed on a Thermo Scientific ESCA-Lab-200i-XL spectrometer (Waltham, MA) with monochromatic Al K $\alpha$  radiation (1486.6 eV), and the C 1s and N 1s peak

spectra were analyzed using XPS Peak 4.1 software. Zeta potential was determined using dynamic light scattering (DLS) with a NanoBrook omni particle sizer and phase-alternative light scattering (PALS) with a zeta potential analyzer, respectively.

The UV-Vis DRS studies of NC-MIL-125-NH<sub>2</sub> were carried out with a Shimadzu UV-2550 UV-Vis spectrophotometer in the wavelength range of 200–800 nm with BaSO<sub>4</sub> as the reference for baseline correction. With the help of the Kubelka-Munk Function, the reflectance data were further converted into absorption terms. The periodic on/off photocurrent responses, the electrochemical impedance spectra (EIS) and the Mott-Schottky plot were recorded using a three-electrode quartz cell on a CHI 660E electrochemical workstation (CH Instrument, USA). For the periodic on/off photocurrent responses, the catalyst dispersed on indium tin oxide (ITO) glass acted as the working electrode, and a Pt flake and Ag/AgCl (saturated KCl) were used as the counter and reference electrode, respectively. The electrolyte was 0.1 M Na<sub>2</sub>SO<sub>4</sub> solution, and the light source was a 250 W xenon high-brightness cold light source (XD-300) equipped with a UV cut-off filter ( $\lambda > 400$  nm). The electrochemical impedance spectra (EIS) was recorded with an alternating current (ac) voltage magnitude of 5 mV over a frequency range of 10<sup>6</sup>–10<sup>-5</sup> Hz in the dark. The Mott-Schottky plot was performed in 0.1 mol/L<sup>-1</sup> Na<sub>2</sub>SO<sub>4</sub> (pH=6.8) with frequencies of 1000 Hz. The catalyst dispersed on fluorine-doped tin oxide (FTO) glass acted as the working electrode. The voltage was scanned from the open-circuit to 1.0 V. The position of conduction band was approximately equal to the flat band. So the conduction band was gotten from the Mott-Schottky analysis by the extrapolation Mott-Schottky plot which intersect at X-axis. The active radical was examined by a Bruker model of electron spin resonance (ESR) employing 5,5-dimethyl-1-pyrroline N-oxide (DMPO) as the spin trapper. Typically, NC-MIL-125-NH<sub>2</sub> (30 mg) was added in a 80 mM DMPO solution with aqueous dispersion for DMPO-·OH and methanol dispersion for DMPO-·O<sub>2</sub><sup>-</sup>. without and with irradiation under the Xenon lamp with an AM1.5, 100mW/cm<sup>2</sup> filter.

**Adsorption Experiments.** Phenolic molecules p-nitrophenol (99%+, J&K Chemical),

phenol (99.5%+, Aladdin Co. Ltd.) and p-methylphenol (99.5%+, Aladdin Co. Ltd.) were selected. Batch adsorption experiments were performed in PTFE screw cap vials sealed with tin foil at  $25 \pm 1$  °C; 60 mL vials were used for NC-MIL-125-NH<sub>2</sub>. Each point, either the blank or calibration control, was evaluated in duplicate. NC-MIL-125-NH<sub>2</sub> was used as an adsorbent in the liquid phase, and the NC-MIL-125-NH<sub>2</sub> powders were prepared into a background solution containing 0.01 mol/L CaCl<sub>2</sub> in deionized water with 200 mg/L NaN<sub>3</sub> as a bio-inhibitor followed by ultrasonication to stabilize the dispersed solution.

The adsorption kinetic studies were conducted with an initial p-nitrophenol, phenol or p-methylphenol concentration of 10 mg/L (0.072 mmol/L for p-nitrophenol, 0.106 mmol/L for phenol, 0.093 mmol/L for p-methylphenol). And the solid-to-water ratios for NC-MIL-125-NH<sub>2</sub> were 1 mg per 50 mL. The remaining concentrations in a series of independent samples were measured from 10 s to 1800 s. Isotherm experiments were performed with solid-to-water ratios at 1 mg of NC-MIL-125-NH<sub>2</sub> samples and 50 mL of p-nitrophenol, phenol or p-methylphenol solution. The initial concentrations of solutions were controlled to obtain equilibrium concentration ranges 0.5-20 mg/L for all three phenolics (0.004 mmol/L- 0.144 mmol/L for p-nitrophenol, 0.005 mmol/L -0.213 mmol/L for phenol, 0.005 mmol/L- 0.185 mmol/L for p-methylphenol). The vials were placed on a shaker and agitated in the dark at 120 rpm for 4 h. The solution was separated from the solid by filtering with 0.22 μm membrane filters. Then, 500 μL of the supernatants were mixed with 500 μL of methanol to determine the p-nitrophenol, phenol and p-methylphenol concentration on an Agilent 1200 HPLC (Agilent Eclipse XDB-C 18 column, 4.6 mm × 250 mm × 5 μm) equipped with a G1321A fluorescence detector. The results showed no noticeable mass loss, and the amount of p-nitrophenol, phenol and p-methylphenol adsorbed by the NC-MIL-125-NH<sub>2</sub> was calculated from the difference between the initial and the equilibrium concentrations.

**Kinetic Models.** The pseudo first-order model can be presented as:  $\ln(q_e - q_t) = \ln q_e - k_1 t$  (1),

where  $k_1$  is the rate constant of the pseudo first-order model of adsorption (1/h);  $q_e$  and  $q_t$  is the absorbed amount of naphthalene at equilibrium and at different time (mg/g), respectively. The values of  $k_1$  and  $q_e$  can be determined from the slope and intercept of linear fittings of  $\ln(q_e - q_t)$  versus  $t$ .

The pseudo second-order model is given by:

$$t/q_t = 1/k_2 q_e^2 + t/q_e \quad (2)$$

where  $k_2$  is the rate constant of the pseudo second-order model of adsorption (g/(mg·h)), while  $q_e$  and  $q_t$  are defined the same as the parameters in the pseudo first-order model. The values of  $k_2$  and  $q_e$  can be determined from the slope and intercept of linear fittings of  $t/q_t$  versus  $t$ .

**Adsorption Models.** The Langmuir and Freundlich models were utilized to fit the adsorption isotherms.

The following expression describes the Langmuir equation:

$$q_e = q_m C_e / (K_L + C_e) \quad (3)$$

where  $q_e$  (mg/g) is the equilibrium-sorbed concentration,  $C_e$  (mg/L) is the equilibrium solution phase concentration,  $K_L$  (L/g) is the Langmuir constant, and  $q_m$  (mg/g) represents the maximum adsorption capacity of the adsorbent.

$$R_L = 1 / (1 + K_L C_0) \quad (4)$$

where  $K_L$  (L/g) is the Langmuir constant and  $C_0$  (g/L) is the initial concentration.  $R_L$  is a dimensionless parameter used to better show the progression of adsorption.

The following expression describes the Freundlich equation:

$$q_e = K_f C_e^N \quad (5)$$

where  $K_f$  [(mg/g)/(mg/L)<sup>N</sup>] is the Freundlich affinity coefficient, and  $N$  is the exponential coefficient.

**Percentage Regenerated.** The percentage regenerated can be presented as:

$$R = q_{n+1} / q_n \quad (6)$$

where  $R$  means the percentage regenerated of the adsorption capacity,  $q_n$  is adsorption capacity in cycle  $n$ .



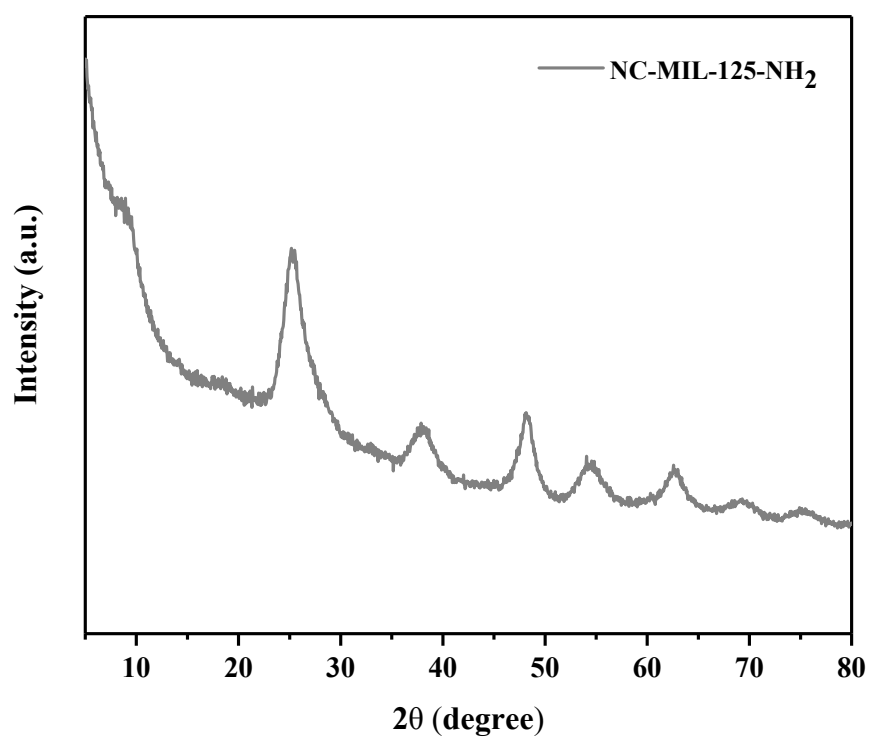


**Figure S-1.** XRD of NC-MIL-125-NH<sub>2</sub>.

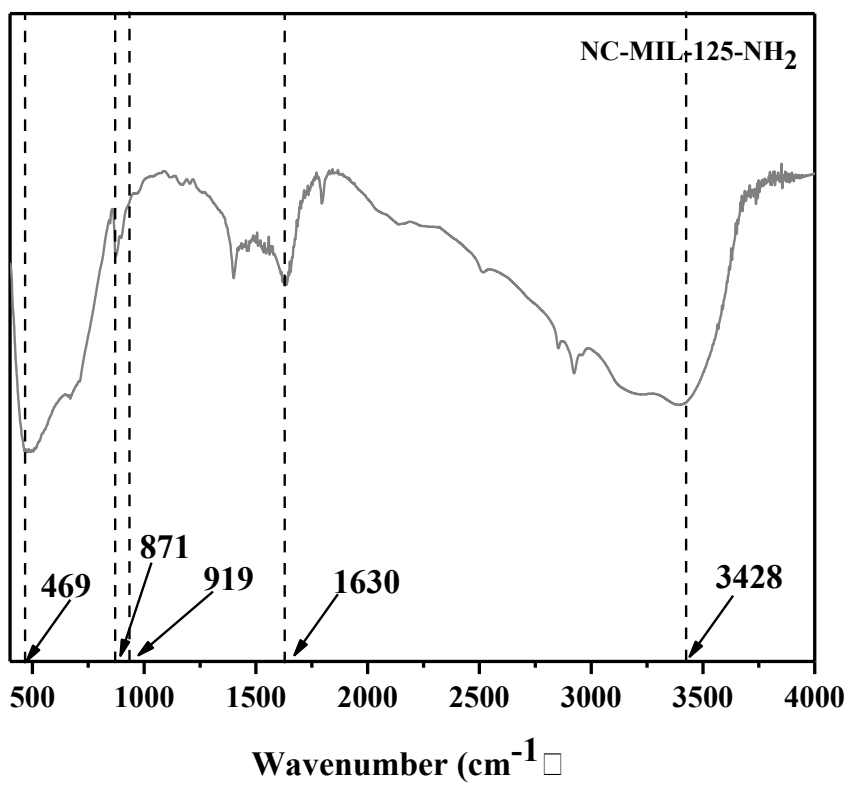
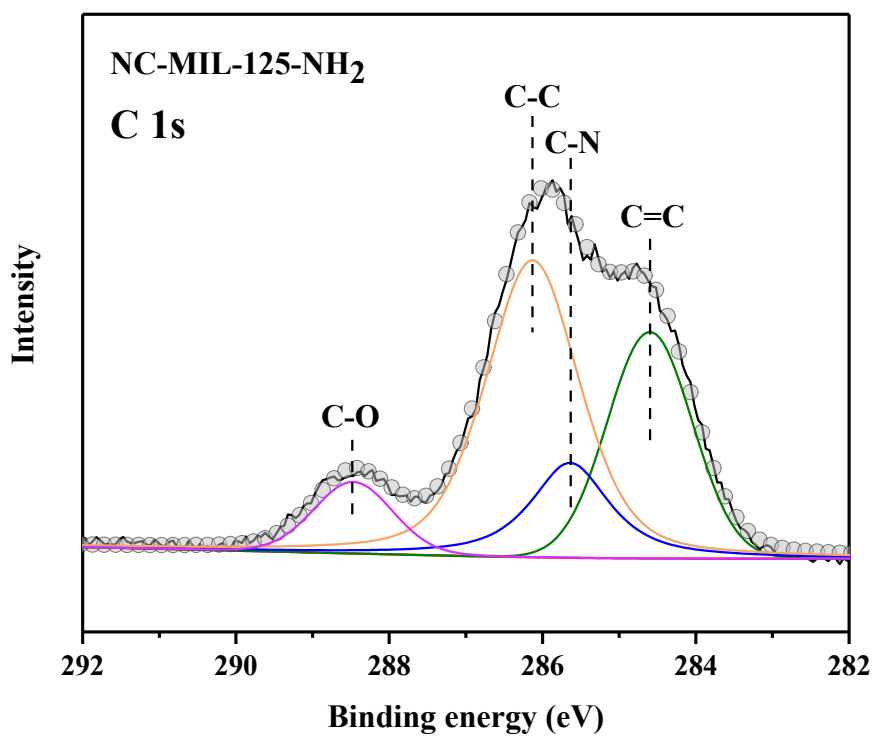
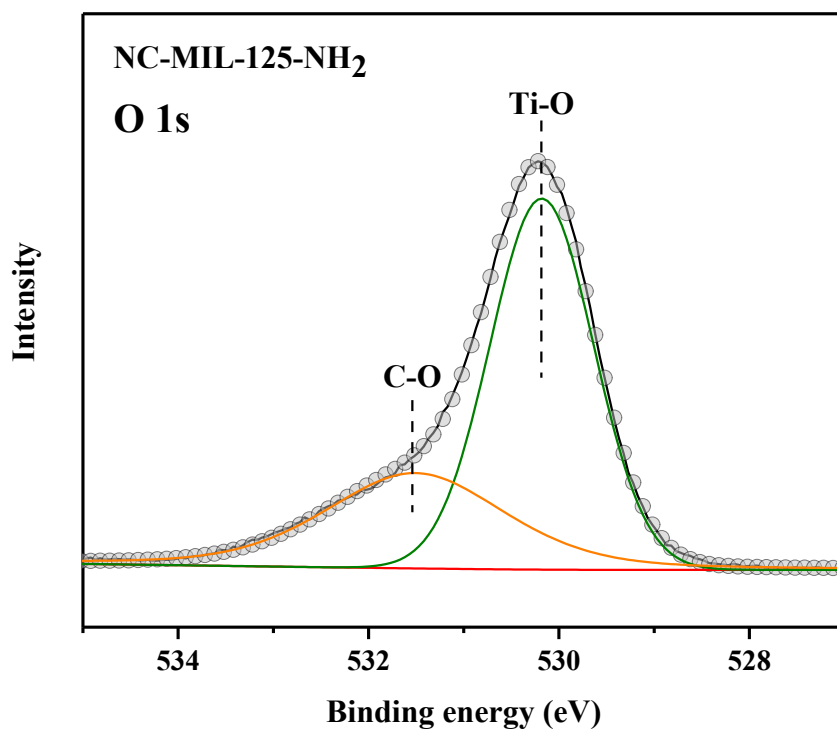


Figure S-2. FTIR of NC-MIL-125-NH<sub>2</sub>.



**Figure S-3.** C 1s of NC-MIL-125-NH<sub>2</sub>.

The C 1s XPS spectrum presented four peaks at 284.60 eV, 285.64 eV, 286.13 eV, and 288.47 eV, corresponding to C=C, C-N, C-C and C-O, respectively. The presence of C=C was attributed to the benzene rings in the linker 2-aminoterephthalic acid (2-NH<sub>2</sub>BDC).



**Figure S-4.** O 1s of NC-MIL-125-NH<sub>2</sub>.

The O 1s XPS spectrum exhibited the band characteristic of lattice oxygen from the titanium-oxo cluster of NC-MIL-125-NH<sub>2</sub> centered at 530.18 eV.

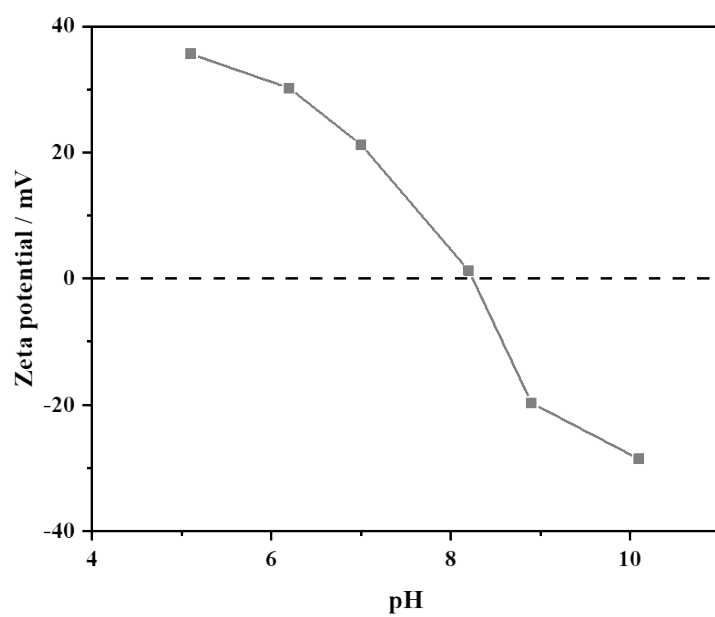
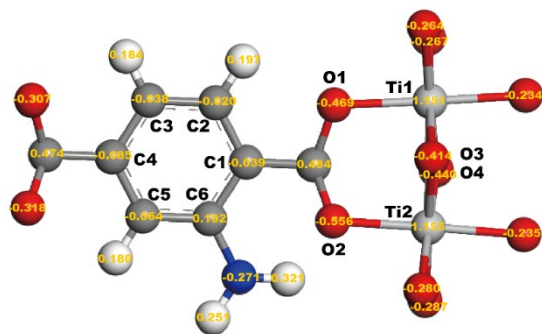
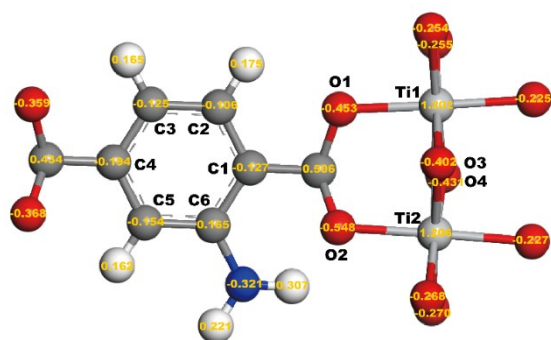


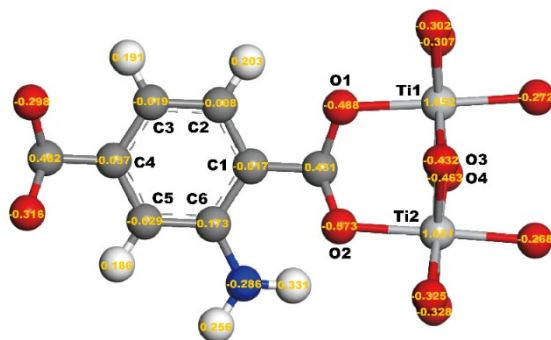
**Figure S-5.** Zeta potential of NC-MIL-125-NH<sub>2</sub>.



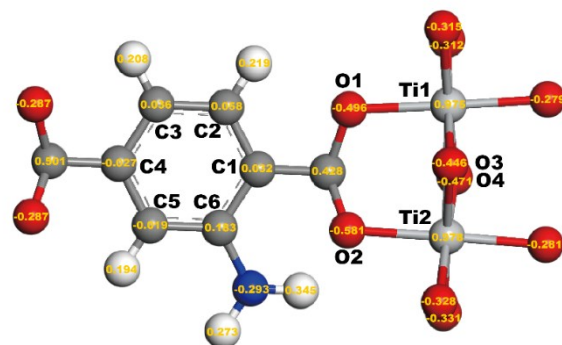
(a)



(b)



(c)



(d)

**Figure S-6.** Charge distribution of the NC-MIL-125-NH<sub>2</sub> matrix in (a) original sample, (b) A-np/NC-MIL-125-NH<sub>2</sub>, (c) A-p/NC-MIL-125-NH<sub>2</sub> and (d) A-mp/NC-MIL-125-NH<sub>2</sub> with the Mulliken charge values of the atoms.

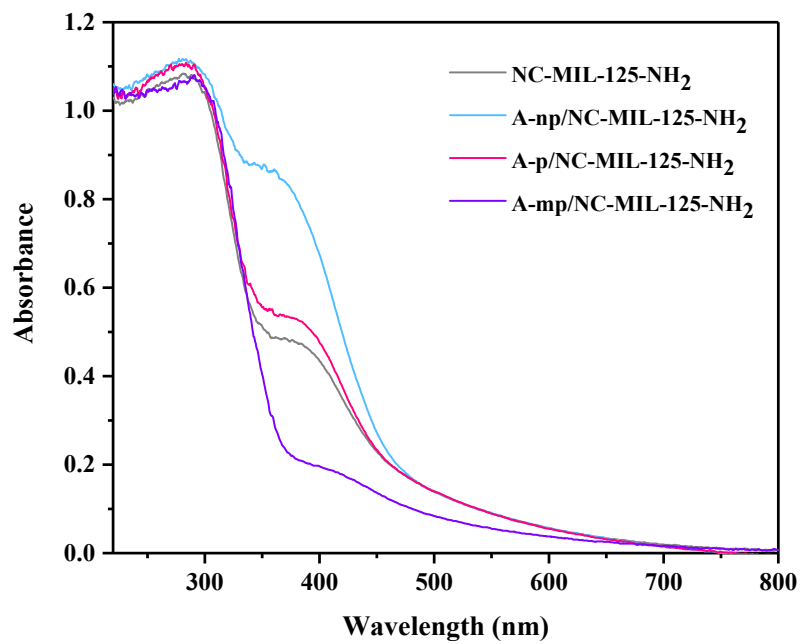


**Figure S-7.** UV-Vis Diffuse Reflection Spectra of NC-MIL-125-NH<sub>2</sub>, A-np/NC-MIL-125-NH<sub>2</sub>, A-p/NC-MIL-125-NH<sub>2</sub> and A-mp/NC-MIL-125-NH<sub>2</sub>.

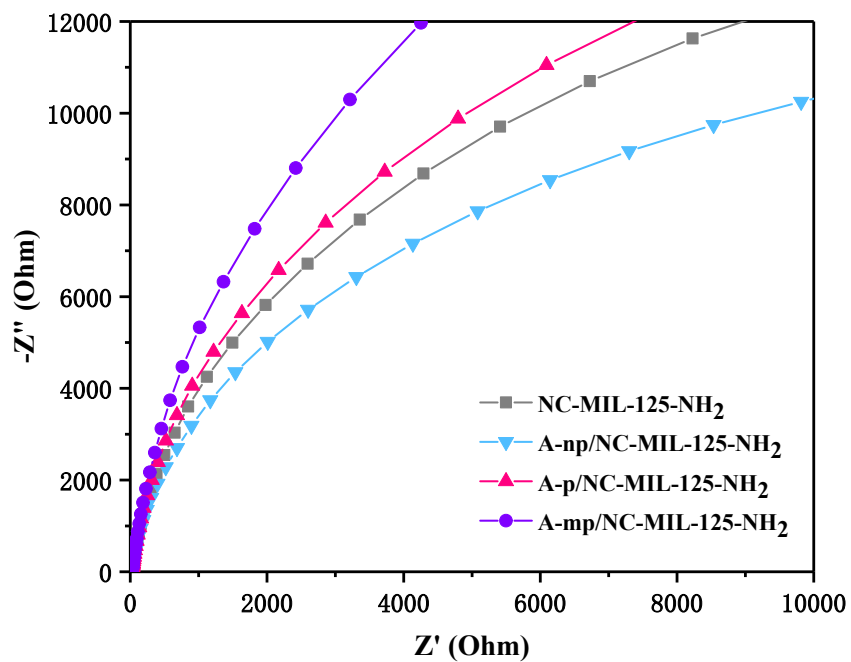


**Figure S-8.** The resistance of charge transfer (RCT) recorded by EIS of NC-MIL-125-NH<sub>2</sub>, A-np/NC-MIL-125-NH<sub>2</sub>, A-p/NC-MIL-125-NH<sub>2</sub> and A-mp/NC-MIL-125-NH<sub>2</sub>.

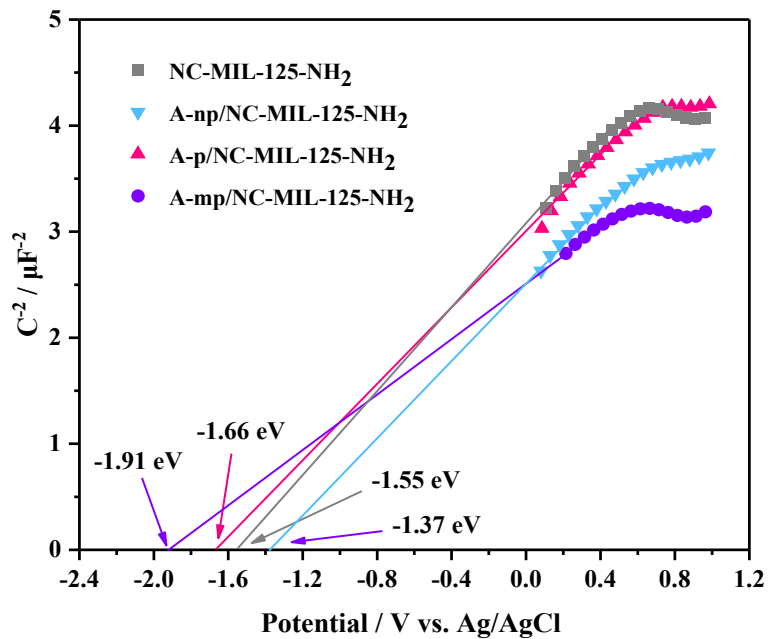


**Figure S-9.** The typical Mott-Schottky plots (scatters) and simulation (lines) of NC-MIL-125-NH<sub>2</sub>, A-np/NC-MIL-125-NH<sub>2</sub>, A-p/NC-MIL-125-NH<sub>2</sub> and A-mp/NC-MIL-125-NH<sub>2</sub>.

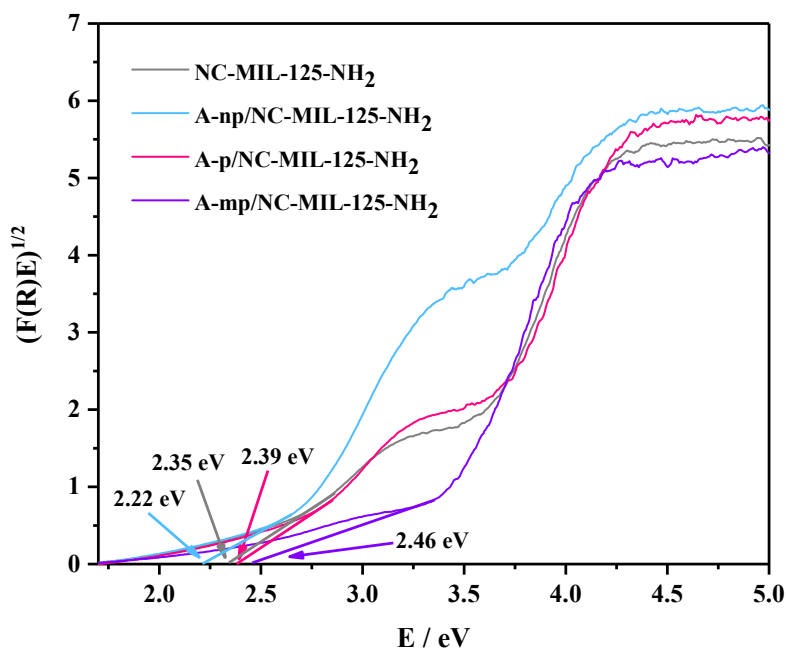


**Figure S-10.** Kubelka–Munk-transformed reflectance spectra of NC-MIL-125-NH<sub>2</sub>, A-np/NC-MIL-125-NH<sub>2</sub>, A-p/NC-MIL-125-NH<sub>2</sub> and A-mp/NC-MIL-125-NH<sub>2</sub>.

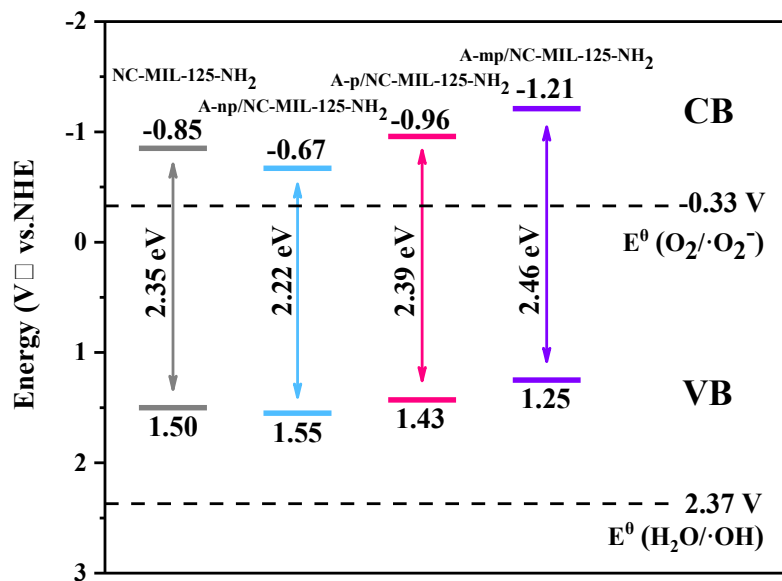


**Figure S-11.** Energy band structure ( $E_{\text{CB}}$  vs. NHE was calculated from  $E_{\text{CB}}$  vs. Ag/AgCl) of NC-MIL-125-NH<sub>2</sub>, A-np/NC-MIL-125-NH<sub>2</sub>, A-p/NC-MIL-125-NH<sub>2</sub> and A-mp/NC-MIL-125-NH<sub>2</sub>.

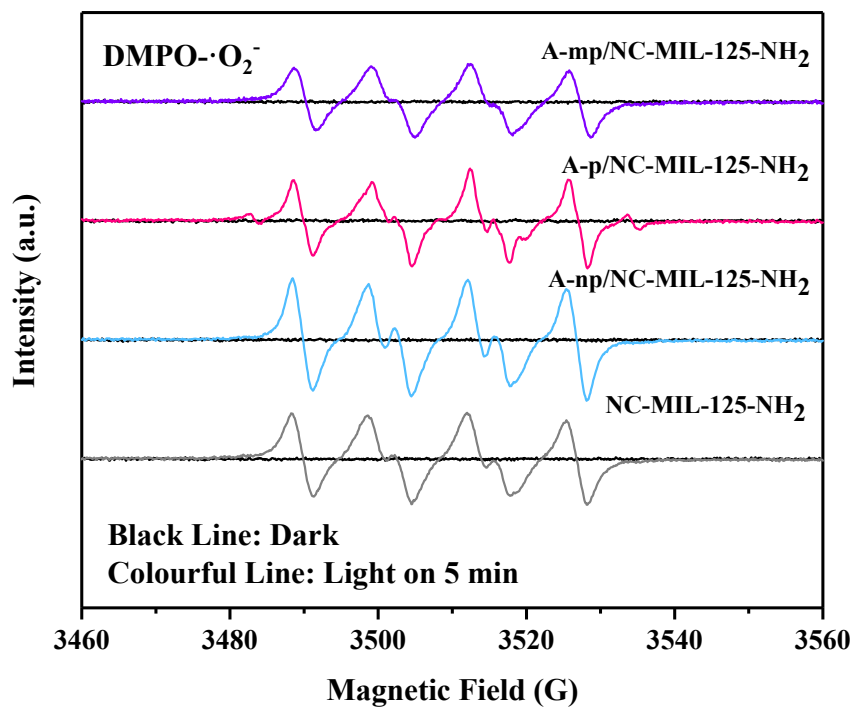


**Figure S-12.** DMPO spin-trapping ESR spectra of NC-MIL-125-NH<sub>2</sub>, A-np/NC-MIL-125-NH<sub>2</sub>, A-p/NC-MIL-125-NH<sub>2</sub> and A-mp/NC-MIL-125-NH<sub>2</sub> in methanol dispersion for DMPO- $\cdot\text{O}_2^-$ .

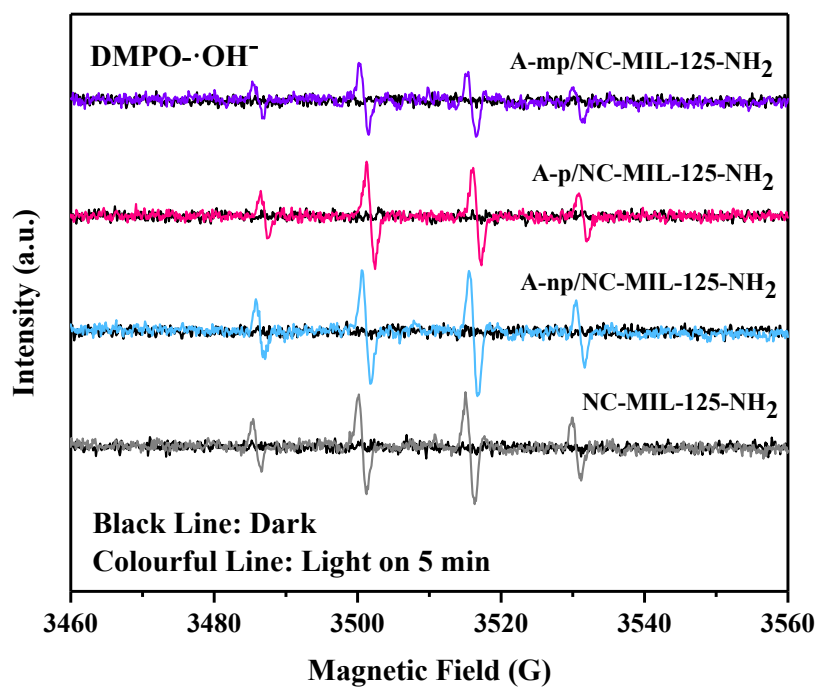


**Figure S-13.** DMPO spin-trapping ESR spectra of NC-MIL-125-NH<sub>2</sub>, A-np/NC-MIL-125-NH<sub>2</sub>, A-p/NC-MIL-125-NH<sub>2</sub> and A-mp/NC-MIL-125-NH<sub>2</sub> in aqueous dispersion for DMPO-·OH.

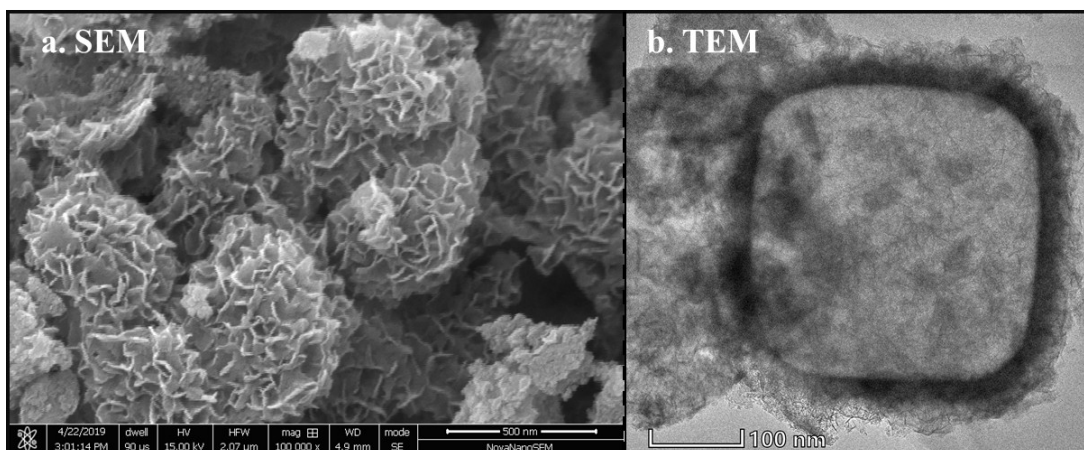


**Figure S-14.** Morphology and structure of A-np/NC-MIL-125-NH<sub>2</sub>. (a) SEM image. Scale bar, 500 nm. (b) TEM image. Scale bar, 100 nm.

According to the comparison of SEM and TEM images (Figure 1(a), 1(b)), the morphology of A-np/NC-MIL-125-NH<sub>2</sub> seemed to be unaltered with NC-MIL-125-NH<sub>2</sub>, which still showed assembled-sheet porous cage-like structures. It meant that the changes in structural morphology of NC-MIL-125-NH<sub>2</sub> before and after were insignificant.

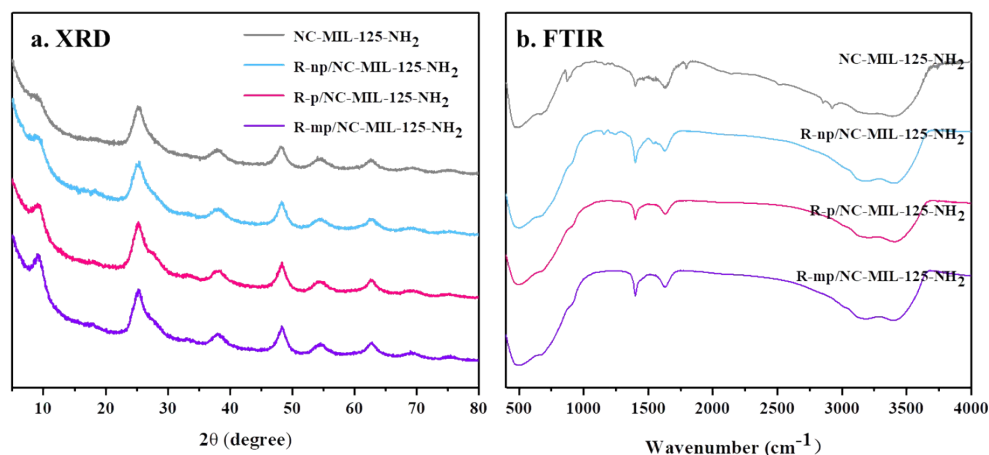


**Figure S-15.** Morphology and structure of NC-MIL-125-NH<sub>2</sub>, R-np/NC-MIL-125-NH<sub>2</sub>, R-p/NC-MIL-125-NH<sub>2</sub> and R-mp/NC-MIL-125-NH<sub>2</sub>. (a) XRD. (b) FTIR spectra.

From the XRD pattern (Figure S-15(a)), R-np/NC-MIL-125-NH<sub>2</sub>, R-p/NC-MIL-125-NH<sub>2</sub> and R-mp/NC-MIL-125-NH<sub>2</sub> exhibited the diffraction peaks of MIL-125-NH<sub>2</sub> as well, which were same to original NC-MIL-125-NH<sub>2</sub>. As to the FTIR spectrum (Figure S-15(b)), there were still typical vibrational bands of Ti–O–Ti–O, –NH<sub>2</sub>, C–N and benzene rings present in the samples of R-np/NC-MIL-125-NH<sub>2</sub>, R-p/NC-MIL-125-NH<sub>2</sub> and R-mp/NC-MIL-125-NH<sub>2</sub>, which indicated NC-MIL-125-NH<sub>2</sub> after regeneration maintained well. The results indicated there were no obvious changes in crystal structure and surface property of NC-MIL-125-NH<sub>2</sub> before and after photocatalytic regeneration, demonstrating the good stability of NC-MIL-125-NH<sub>2</sub>.

**Table S-1. The Content of Chemical Bonds in NC-MIL-125-NH<sub>2</sub> Derived from XPS Data.**

NC-MIL-125-NH <sub>2</sub>		
C 1s		
	C=C (%)	27.98
	C-N (%)	15.08
	C-C (%)	48.39
	C-O (%)	8.55
N 1s		
	-NH <sub>2</sub> (%)	24.45
	-N=+ (%)	21.40
	-N-+ (%)	54.15
O 1s		
	Ti-O (%)	65.90
	C-O (%)	34.10
Ti 2p		
	Ti 2p <sub>3/2</sub> (%)	68.57
	Ti 2p <sub>1/2</sub> (%)	31.43

**Table S-2. Adsorption Kinetic Parameters of p-Nitrophenol, Phenol and p-Methylphenol onto NC-MIL-125-NH<sub>2</sub>.<sup>a)</sup>**

Phenolics	Pseudo first-order			Pseudo second-order		
	$q_e$ (mmol/g)	$k_1$ (1/s)	$R^2$	$q_e$ (mmol/g)	$k_2$ (g/(mmol·s))	$R^2$
p-nitrophenol	0.670	0.017	0.989	0.758	0.023	0.955
phenol	0.371	0.015	0.995	0.411	0.020	0.973
p-methylphenol	0.245	0.009	0.988	0.269	0.012	0.983

a) The solid solution ratio was 1 mg/50 mL. All of the initial concentrations of p-nitrophenol, phenol and p-methylphenol were 0.072, 0.106 and 0.093 mmol/L, respectively.

**Table S-3. Regression Parameters of Adsorption Isotherms of p-Nitrophenol, Phenol and p-Methylphenol onto NC-MIL-125-NH<sub>2</sub> Fitted by the Freundlich and Langmuir Models.**

Phenolics	Freundlich Model			Langmuir Model			
	$K_f$ ((mmol/g)/(mmol/L) <sup>1/n</sup> )	$N$	$R^2$	$q_m$ (mmol/g)	$K_L$ (L/g)	$R_L$	$R^2$
p-nitrophenol	2.128	0.499	0.863	0.916	27.662	0.644	0.930
phenol	0.758	0.364	0.790	0.454	35.402	0.586	0.927
p-methylphenol	0.817	0.571	0.864	0.420	12.945	0.794	0.929

**Table S-4. The Percentage Regenerated of Adsorption Capacity for NC-MIL-125-NH<sub>2</sub> in the Timeline of Photocatalytic Regeneration.**

	Recovery (%)					
	0.5 h	1 h	1.5 h	2 h	3 h	5 h
p-nitrophenol	30.14	60.01	75.74	86.87	96.19	98.96
phenol	26.25	53.54	70.34	81.26	91.79	97.85
p-methylphenol	23.86	47.39	63.93	73.82	85.40	94.28

**Table S-5. The Percentage Regenerated of Adsorption Capacity for NC-MIL-125-NH<sub>2</sub> in the 2<sup>nd</sup>, 3<sup>rd</sup> and 4<sup>th</sup> Cycle of Photocatalytic Regeneration.**

	Recovery (%)		
	2 <sup>nd</sup>	3 <sup>rd</sup>	4 <sup>th</sup>
p-nitrophenol	98.96	98.04	97.45
phenol	97.85	96.38	95.49
p-methylphenol	94.28	93.65	91.35

**Table S-6. Standardizing  $\Delta i_{\text{photo}}$  by Adsorption Capacities.**

	$q_m$ (mmol/g)		$i_{\text{photo}}$ ( $\mu\text{A}/\text{cm}^2$ )	$\Delta i_{\text{photo}}/q_m$ <sup>a)</sup> ( $(\mu\text{A}\cdot\text{g})/(\text{mmol}\cdot\text{cm}^2)$ )
		NC-MIL-125-NH <sub>2</sub>	5.2	
p-nitrophenol	0.916	A-np/NC-MIL-125-NH <sub>2</sub>	8.2	3.277
phenol	0.454	A-p/NC-MIL-125-NH <sub>2</sub>	5.0	-0.441
p-methylphenol	0.420	A-mp/NC-MIL-125-NH <sub>2</sub>	3.7	-3.574

a)  $\Delta i_{\text{photo}}$  is the value that  $i_{\text{photo}}$  of NC-MIL-125-NH<sub>2</sub> after adsorption minus  $i_{\text{photo}}$  of original NC-MIL-125-NH<sub>2</sub>.